Farnesoid X Receptor Deficiency Improves Glucose Homeostasis in Mouse Models of Obesity

Janne Prawitt,[1] Mouaadh Abdelkarim,[1] Johanna H.M. Stroeve,[2] Iuliana Popescu,[1] Helene Duez,[1] Vidya R. Velagapudi,[3] Julie Dumont,[1] Emmanuel Bouchaert,[1] Theo H. van Dijk,[2] Anthony Lucas,[1] Emilie Dorchies,[1] Mehdi Daoudi,[1] Sophie Lestavel,[1] Frank J. Gonzalez,[4] Matej Oresic,[3] Bertrand Cariou,[1,5] Folkert Kuipers,[2] Sandrine Caron,[1] and Bart Staels[1]

OBJECTIVE—Bile acids (BA) participate in the maintenance of metabolic homeostasis acting through different signaling pathways. The nuclear BA receptor farnesoid X receptor (FXR) regulates pathways in BA, lipid, glucose, and energy metabolism, which become dysregulated in obesity. However, the role of FXR in obesity and associated complications, such as dyslipidemia and insulin resistance, has not been directly assessed.

RESEARCH DESIGN AND METHODS—Here, we evaluate the consequences of FXR deficiency on body weight development, lipid metabolism, and insulin resistance in murine models of genetic and diet-induced obesity.

RESULTS—FXR deficiency attenuated body weight gain and reduced adipose tissue mass in both models. Surprisingly, glucose homeostasis improved as a result of an enhanced glucose clearance and adipose tissue insulin sensitivity. In contrast, hepatic insulin sensitivity did not change, and liver steatosis aggravated as a result of the repression of β-oxidation genes. In agreement, liver-specific FXR deficiency did not protect from diet-induced obesity and insulin resistance, indicating a role for nonhepatic FXR in the control of glucose homeostasis in obesity. Decreasing elevated plasma BA concentrations in obese FXR-deficient mice by administration of the BA sequestrant colesevelam improved glucose homeostasis in a FXR-dependent manner, indicating that the observed improvements by FXR deficiency are not a result of indirect effects of altered BA metabolism.

CONCLUSIONS—Overall, FXR deficiency in obesity beneficially affects body weight development and glucose homeostasis. ***Diabetes*** **60:1861–1871, 2011**

Obesity is characterized by an excess of adipose tissue mass, which predisposes to metabolic perturbations, including insulin resistance, hyperlipidemia, and fatty liver, promoting the development of type 2 diabetes and cardiovascular disease. Dysregulation of various metabolic pathways in tissues such as adipose tissue, skeletal muscle, pancreas, and liver lies at the basis of these metabolic complications, but the exact mechanisms are still not well understood (1).

Nuclear receptors are ligand-activated transcription factors, which regulate gene expression by binding to specific response elements in the promoters of target genes. The farnesoid X receptor (FXR) is a key regulator of bile acid (BA) metabolism. By promoting BA efflux from the liver, inhibiting hepatic BA synthesis and intestinal absorption, FXR controls the enterohepatic cycling of BA (2). Additionally, FXR regulates lipid metabolism, insulin sensitivity, and energy homeostasis (3). FXR activation lowers plasma and liver triglycerides by repressing sterol regulatory element–binding protein (SREBP)1c-mediated hepatic lipogenesis (4) and by enhancing plasma triglyceride clearance via apolipoprotein (apo)CII induction (5) and apoCIII inhibition (6) in the liver, resulting in an increased lipoprotein lipase (LPL) activity. Consequently, FXR-deficient ($FXR^{-/-}$) mice are dyslipidemic, displaying elevated plasma triglycerides and total and HDL cholesterol (7–9).

The characterization of $FXR^{-/-}$ mice further revealed an important function of FXR in the control of glucose homeostasis. $FXR^{-/-}$ mice are transiently hypoglycemic when fasted (8,10) and exhibit a delayed intestinal glucose absorption (10) and a reduced hepatic glycogen content (10–12). Hepatic gluconeogenic gene expression is decreased in the absence of FXR (11–13) and induced upon FXR activation in vivo (14). Moreover, $FXR^{-/-}$ mice display peripheral insulin resistance with an impaired insulin signaling response in adipose tissue and skeletal muscle (8,13). Additionally, FXR may control adipose tissue biology. $FXR^{-/-}$ mice exhibit a decrease in adipose tissue mass with smaller adipocytes (8). Conversely, FXR activation in vitro stimulates adipocyte differentiation (15) by promoting peroxisome proliferator–activated receptor (PPAR)-γ activity and inhibiting the Wnt/β-catenin pathway (16).

BA act as regulators of metabolic homeostasis also through FXR-independent pathways (17). Apart from FXR, BA have been reported to activate the G protein–coupled BA receptor (TGR5), the pregnane X receptor (PXR), the vitamin D receptor (VDR), or the formyl peptide receptor (FPR) (17). TGR5 activation by BA increases energy expenditure in thermogenic tissues by inducing deiodinase 2 (D2) (18) and improves glucose homeostasis by stimulating glucagon-like peptide 1 (GLP-1) secretion from intestinal L cells (19,20). Hence, because FXR controls plasma BA concentrations, the metabolic actions of FXR can be a result of direct FXR-mediated and/or indirect BA-mediated effects (2). BA metabolism can be pharmacologically modulated by BA sequestrants (BAS), such as colesevelam, which bind BA in the intestinal lumen and interrupt their

From the [1]University of Lille Nord de France; INSERM UMR1011; UDSL; Institut Pasteur de Lille, Lille, France; the [2]Center for Liver, Digestive and Metabolic Diseases, Laboratory of Pediatrics, University Medical Center Groningen, Groningen, the Netherlands; the [3]VTT Technical Research Centre of Finland, Espoo, Finland; the [4]Laboratory of Metabolism, Center for Cancer Research, National Cancer Institute, National Institutes of Health, Bethesda, Maryland; and [5]INSERM U915; Faculty of Medicine, University of Nantes, Thorax Institute; Clinic of Endocrinology, University Hospital Center Nantes, Nantes, France.

Corresponding author: Bart Staels, bart.staels@pasteur-lille.fr.

Received 11 January 2011 and accepted 3 April 2011.

DOI: 10.2337/db11-0030

This article contains Supplementary Data online at http://diabetes.diabetesjournals.org/lookup/suppl/doi:10.2337/db11-0030/-/DC1.

enterohepatic cycling. BAS lower plasma cholesterol levels by stimulating hepatic BA synthesis from cholesterol and increasing LDL receptor activity (3). In diabetic patients, BAS improve glycemic control (21), associated with an activation of the incretin system as a result of an enhanced GLP-1 secretion as shown in rodent models of diabetes (22,23).

Studies on the metabolic function of FXR have so far been limited to lean $FXR^{-/-}$ mice. However, the role of FXR in the adaptation to obesity and its metabolic complications has not yet been assessed. To address this issue, we investigated the impact of FXR deficiency in murine models of genetic (*ob/ob*) and diet-induced obesity. Our results show that FXR deficiency protects from excessive body weight gain in both models by reducing adipose tissue mass. Interestingly, hyperglycemia and glucose tolerance improved, associated with improved peripheral glucose clearance and adipose tissue insulin sensitivity. Liver insulin sensitivity was not altered by FXR deficiency, and hepatic steatosis became even more pronounced, associated with elevated plasma triglyceride levels and reduced expression of genes implicated in β-oxidation. Furthermore, liver-specific FXR-deficient mice were not protected from diet-induced obesity and insulin resistance, indicating a role for nonhepatic FXR in the improvement of glucose metabolism. Finally, to assess the contribution of elevated plasma BA concentrations observed in FXR-deficient models of obesity, plasma BA levels were reduced by administration of the BAS colesevelam. Colesevelam treatment improved glucose homeostasis in genetic obesity only in the presence of FXR, indicating that the changes in BA concentrations are not responsible for the improved glucose homeostasis in obese $FXR^{-/-}$ mice. Thus, selective FXR antagonism or elimination of ligands, e.g., by BAS, may be an interesting pharmacological option for the therapy of metabolic disorders associated with obesity.

RESEARCH DESIGN AND METHODS

Animals. All experiments were performed with the approval of the Institut Pasteur de Lille review board. Animals were housed in a 12-h light/12-h dark cycle and maintained on standard chow (A0; SAFE). Unless stated otherwise, male mice were used for experimentation. $FXR^{-/-}$ (7) and FXR-floxed mice (7) were backcrossed for 7 or 10 generations, respectively, onto a C57Bl/6 J background. $FXR^{+/+}$*ob/ob* and $FXR^{-/-}$*ob/ob* mice and lean littermates were generated by crossing $FXR^{-/-}$ and leptin-deficient mice (B6.V-Lep^{ob}/J; Charles River). Liver-specific $FXR^{-/-}$ mice ($FXR^{flox/flox}$Alb-$Cre^{+/-}$=$LFXR^{-/-}$) and wild-type littermates ($FXR^{flox/flox}$Alb-$Cre^{-/-}$=$LFXR^{+/+}$) were generated by crossing FXR-floxed and Albumin-Cre recombinase expressing mice (C57BL/6-Tg[Alb-cre]21Mgn/J; Charles River). To study diet-induced obesity, mice received a high-fat diet (HFD; D12492; Research Diets; 60% kcal fat) and controls received a low-fat diet (D12450B; Research Diets; 10% kcal fat), 20-week-old $FXR^{+/+}$ and $FXR^{-/-}$ mice for 20 weeks and 10-week-old $LFXR^{-/-}$ and $LFXR^{+/+}$ mice for 9 weeks. The BAS colesevelam (Daiichi Sankyo) was administered with the diet (2% in standard chow) ad libitum to 10-week-old $FXR^{+/+}$*ob/ob* and $FXR^{-/-}$*ob/ob* mice for 3 weeks. Body weight was monitored weekly. Fat and lean mass were determined by dual-energy X-ray absorptiometry (Piximus; GE Medical Systems LUNAR). Food intake was estimated during six periods of 2 days. Animals were killed after a 6-h fast by cervical dislocation. Tissues were removed and snap-frozen in liquid nitrogen.

Plasma parameters. Blood was sampled after a 6-h fast, and parameters were determined as follows: blood glucose (Accu-Check; Roche Diagnostics), insulin (Mercodia), nonesterified free fatty acids (FFA; Wako), triglycerides (Biomerieux), leptin (R&D Systems), and total BA, as described (24). Lipoprotein profiles in plasma pools were generated by fast protein liquid chromatography (Superose 6 HR 10/30; Amersham GE Healthcare) with subsequent determination of triglycerides.

Indirect calorimetry. Mice were housed individually in metabolic cages (Oxylet; PanLab) for 48 h to measure O_2 consumption (Vo_2) and CO_2 production (Vco_2). Energy expenditure was calculated as described (25).

VLDL production. Mice were intravenously injected with 500 mg/kg Tyloxapol (Sigma) after a 6-h fast, and triglycerides were measured in plasma sampled as indicated.

Assessment of glucose metabolism. For tolerance tests, 1 g/kg glucose or 2 IU/kg insulin (Actrapid Penfill; Novo Nordisk), respectively, was injected intraperitoneally and blood glucose was measured as indicated. The metabolic clearance rate (MCR) was determined by stable isotope dilution as described (26). To measure the insulin signaling response, tissues were harvested 10 min after intraperitoneal injection of 1 IU/kg insulin (Actrapid Penfill; Novo Nordisk) or 0.9% NaCl into overnight-fasted female mice. Serine473-phosphorylated Akt and total Akt protein expression (Cell Signaling Technology) were detected by Western blot, and signals were quantified by GeneTool software (Syngene). Pancreas morphometry was analyzed as described (27).

Quantitative RT-PCR. Total RNA was isolated from tissues by guanidinium thiocyanate/phenol/chloroform extraction (28) and reverse transcribed into cDNA (Superscript II kit; Applied Bioscience). Quantitative PCR (QPCR) was performed with the BrilliantII SYBR Green QPCR Master Mix (Agilent) and specific primers (Supplementary Table 1) on an mx3005 (Agilent). Gene expression was normalized to 28S, and the value in $FXR^{+/+}$*ob/ob* samples was set to 1.

Lipidomics. Lipidomics analysis of adipose tissue was performed as described (29).

Statistical analysis. All values are reported as means ± SEM. Statistical significance was analyzed as indicated by two-way ANOVA and Bonferroni post hoc test or Mann-Whitney test using Prism (GraphPad). Differences were considered significant when $P < 0.05$. Partial least squares discriminant analysis (PLS/DA) was performed using Matlab, version 7.5 (Mathworks) and PLS Toolbox, version 4.2 (Eigenvector Research).

RESULTS

FXR deficiency attenuates weight gain in genetic obesity. As a first approach to assess the role of FXR in obesity, $FXR^{-/-}$ mice were crossed into the *ob/ob* background to produce $FXR^{-/-}$*ob/ob* mice, which were compared with $FXR^{+/+}$*ob/ob* controls.

The weight gain observed in $FXR^{+/+}$*ob/ob* mice was significantly attenuated by FXR deficiency, already from 7 weeks of age onward (Fig. 1*A*) ($P < 0.0001$; two-way ANOVA). Dual-energy X-ray absorptiometry revealed a decrease in fat (22%) and less pronounced in lean (10%) mass of $FXR^{-/-}$*ob/ob* mice (Fig. 1*B*). Concordantly, the estimated food intake tended to decrease in $FXR^{-/-}$*ob/ob* mice (15.5 ± 1.1 vs. 18.9 ± 0.8 kcal/day/mouse). Indirect calorimetry demonstrated that Vo_2 and Vco_2 were equally reduced in $FXR^{-/-}$*ob/ob* mice compared with $FXR^{+/+}$*ob/ob* controls (Fig. 1*C* and *D*), resulting in nearly identical values for the respiratory quotient (data not shown). Consistent with the decrease in Vo_2 and body weight, calculated energy expenditure was lower in $FXR^{-/-}$*ob/ob* than in $FXR^{+/+}$*ob/ob* mice (7.1 ± 0.3 vs. 8.7 ± 0.7 kcal/day/mouse) even though the difference did not reach statistical significance.

Overall, FXR deficiency leads to a decreased storage of energy in the form of adipose tissue, resulting in a lower total body weight.

FXR deficiency improves glucose homeostasis in genetic obesity by increasing peripheral glucose disposal. Because lean $FXR^{-/-}$ mice develop peripheral insulin resistance (8,13), it was next assessed whether FXR deficiency in obesity affects glucose homeostasis. In contrast with hyperglycemic $FXR^{+/+}$*ob/ob* mice, $FXR^{-/-}$*ob/ob* mice displayed normal blood glucose levels (Fig. 2*A*) ($P < 0.0001$; two-way ANOVA). In addition, the hyperinsulinemia typically observed in $FXR^{+/+}$*ob/ob* mice was significantly reduced in the absence of FXR (Fig. 2*B*). Concordant with the decreased hyperglycemia and hyperinsulinemia, glucose tolerance was significantly improved in $FXR^{-/-}$*ob/ob* mice (Fig. 2*C*), as a result of a combination of lower fasting glycemia and improved glucose handling as evident from the significantly smaller integrated area under the curve (iAUC) (Fig. 2*D*). The MCR of glucose was further

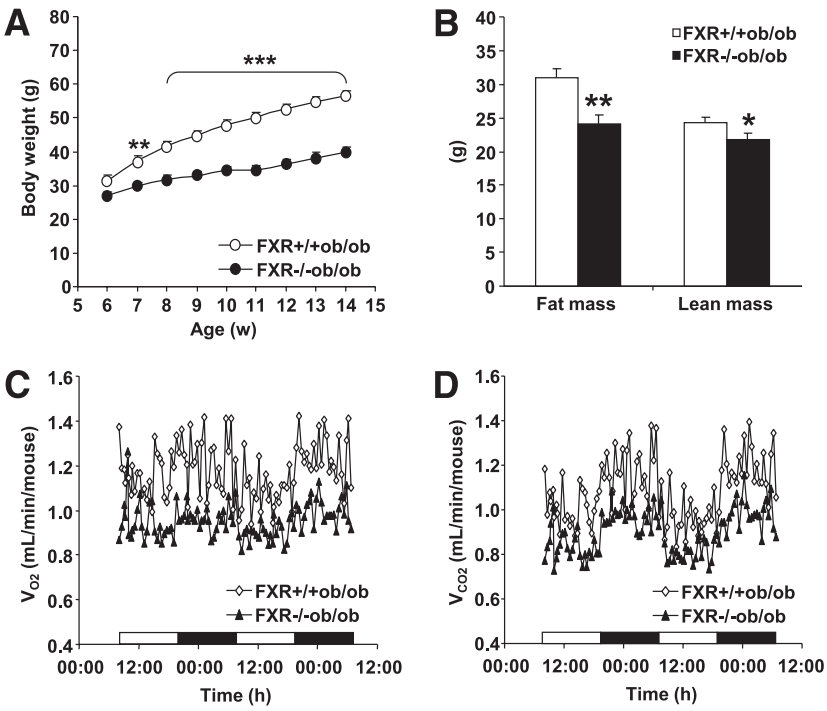

FIG. 1. FXR deficiency attenuates weight gain in *ob/ob* mice. *A*: FXR$^{+/+}$*ob/ob* (white bars and symbols) and FXR$^{-/-}$*ob/ob* mice (black bars and symbols) (n = 9 to 10/group) were monitored weekly for body weight. Significance of the overall effect of genotype ($P < 0.0001$) and age ($P < 0.0001$) as well as their interaction ($P < 0.0001$) was calculated by two-way ANOVA. *B*: Body composition was assessed by dual-energy X-ray absorptiometry in 20-week-old mice (n = 9 to 10/group). Vo_2 (*C*) and Vco_2 (*D*) were determined in 20-week-old mice (n = 5/group) individually housed in metabolic cages. Values are means ± SEM. Differences between genotypes over time were analyzed by two-way ANOVA and Bonferroni post hoc test; differences between genotypes were calculated by Mann-Whitney test (*P = 0.05, **$P < 0.01$, ***$P < 0.001$).

significantly improved in FXR$^{-/-}$*ob/ob* mice (Fig. 2*E*), indicative of a higher glucose disposal in the periphery. In line, an insulin tolerance test showed that FXR$^{-/-}$*ob/ob* mice are more insulin sensitive than FXR$^{+/+}$*ob/ob* mice (Fig. 2*F* and *G*) with a more drastic decline of blood glucose levels in response to the administered insulin bolus ($P < 0.0001$; two-way ANOVA). Insulin-resistant FXR$^{+/+}$*ob/ob* mice exhibited enlarged islets of Langerhans (Fig. 2*H*, compare arrows) because of compensatory hypertrophy. In contrast, islets of FXR$^{-/-}$*ob/ob* mice were significantly smaller (Fig. 2*I*), likely reflecting the relieved metabolic pressure as a result of the improved insulin sensitivity. These findings indicate that, in contrast with lean mice, FXR deficiency might improve glucose homeostasis in genetic obesity.

Adipose tissue, but not hepatic insulin sensitivity, is improved in FXR$^{-/-}$*ob/ob* mice. To analyze the contribution of peripheral tissues and the liver to the improvement of insulin sensitivity, the phosphorylation of Akt, a key mediator of the metabolic action of insulin, was measured in response to an in vivo–administered insulin bolus (Fig. 3*A*). Akt phosphorylation was increased in adipose tissue of FXR$^{-/-}$*ob/ob* compared with FXR$^{+/+}$*ob/ob* mice (2.8× vs. 1.5×). In contrast, the response in skeletal muscle (4.5× vs. 4.8×) and liver (2.0× vs. 1.7×) was not different between genotypes.

Hepatic insulin resistance is often associated with a fatty liver (30). Because FXR regulates lipogenesis in lean mice (2), hepatic gene expression and lipid content were determined. No changes were seen in the mRNA expression of the key regulator of lipogenesis, *SREBP1c* (Fig. 3*B*). Expression of genes involved in FA synthesis was only modestly induced (acethyl CoA carboxylase [*ACC*]*1*, fatty acid synthase [*FAS*], stearoyl CoA desaturase [*SCD*]*1*) in livers of FXR$^{-/-}$*ob/ob* mice (Fig. 3*B*). Nevertheless, the hepatic triglyceride content was doubled in the absence of FXR (Fig. 3*C*). The expression of PPAR-α, a key regulator of FA oxidation, and carnitine palmitoyltransferase (*CPT*)*1A*, which ensures the FA entry into the mitochondria, was significantly decreased in FXR$^{-/-}$*ob/ob* compared with FXR$^{+/+}$*ob/ob* mice (Fig. 3*B*). Expression of *ACC2*, which indirectly inhibits *CPT1A*, was significantly higher, indicating that a reduced FA oxidation likely contributes to the increased steatosis in FXR$^{-/-}$*ob/ob* mice.

Thus, an improvement of adipose tissue insulin sensitivity seems to account for the observed changes in glucose homeostasis. Hepatic insulin sensitivity was not altered by FXR deficiency, even though liver steatosis increased.

FXR$^{-/-}$*ob/ob* mice exhibit hypertriglyceridemia as a result of an impaired intravascular triglyceride clearance. Because FXR$^{-/-}$*ob/ob* mice display increased liver steatosis and reduced adipose tissue mass, it was tested whether this phenotype was associated with alterations in triglyceride or FA metabolism. Plasma FFA concentrations were not different between genotypes (Fig. 4*A*). In contrast, plasma triglyceride levels were strongly elevated in FXR$^{-/-}$*ob/ob* compared with FXR$^{+/+}$*ob/ob* mice (Fig. 4*B*). Analysis of the lipoprotein profile revealed that triglycerides were mainly increased in VLDL, but also intermediate-density lipoprotein (IDL)/LDL-sized particles (Fig. 4*C*). To determine whether this was because of altered hepatic triglyceride secretion, plasma triglyceride accumulation was assessed after inhibition of intravascular lipolysis (Fig. 4*D*). Hepatic VLDL production was similar between FXR$^{-/-}$*ob/ob* and FXR$^{+/+}$*ob/ob* mice, suggesting that an impairment of intravascular triglyceride clearance

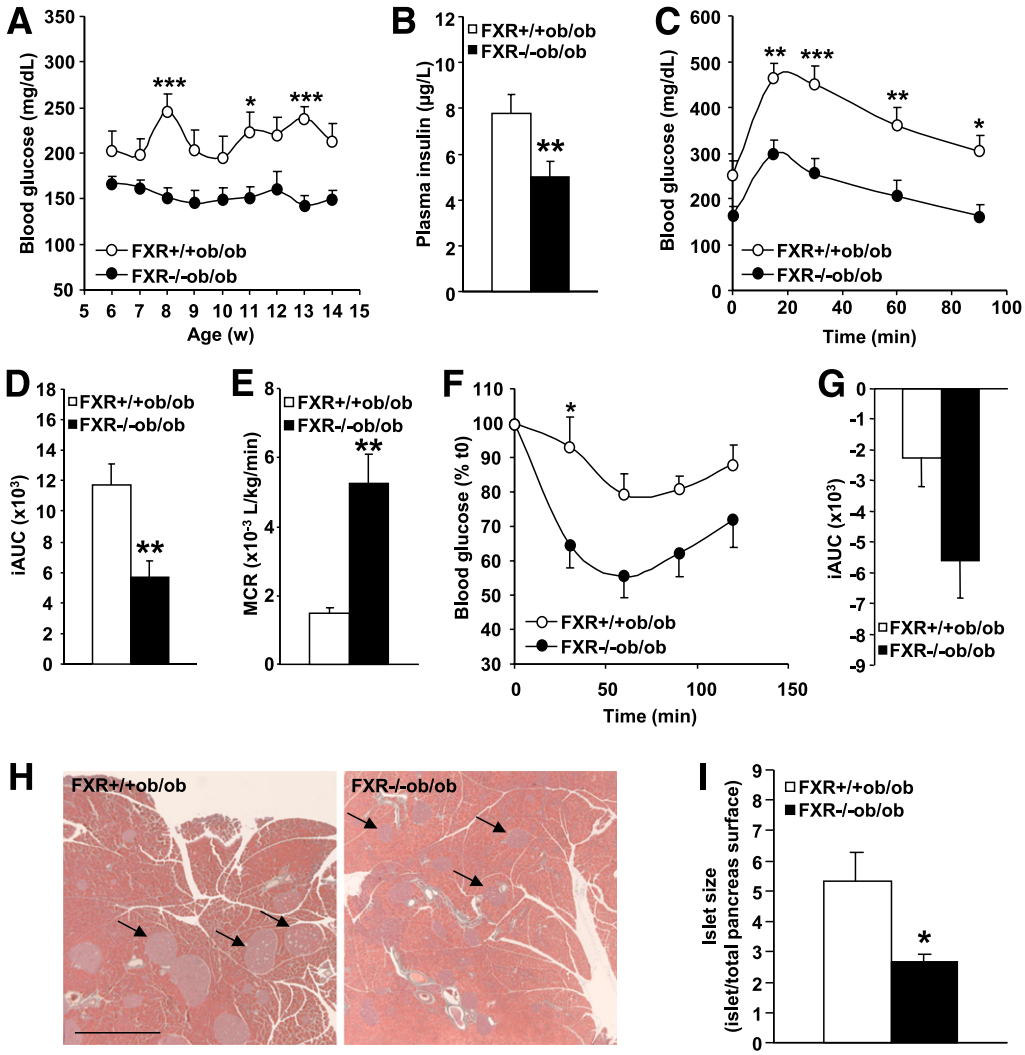

FIG. 2. FXR deficiency improves glucose homeostasis in *ob/ob* mice. *A*: Fasting blood glucose was measured weekly in FXR$^{+/+}$*ob/ob* (white bars or circles) and FXR$^{-/-}$*ob/ob* mice (black bars or circles) (n = 9 to 10/group). Significance of the overall effect of the genotype ($P < 0.0001$) was calculated by two-way ANOVA. *B*: Plasma insulin was determined in 12-week-old mice (n = 9 to 10/group). Blood glucose excursion (*C*) and integrated AUC (*D*) after administration of an intraperitoneal glucose bolus (1 g/kg glucose) were measured in 12-week-old mice (n = 9 to 10/group). Significance of the overall effect of genotype ($P < 0.0001$) and time ($P < 0.0001$) was calculated by two-way ANOVA. *E*: MCR was determined by stable isotope dilution in 14-week-old mice (n = 5 to 6/group). Blood glucose excursion (*F*) and iAUC (*G*) after administration of an intraperitoneal insulin bolus (2 IU insulin/kg) were measured in 13-week-old mice (n = 9 to 10/group). Significance of the overall effect of genotype ($P < 0.0001$) and time ($P < 0.0001$) was calculated by two-way ANOVA. *H*: Pancreata of 20-week-old mice (n = 9 to 10/group) were sectioned and submitted to Papanicolaou staining. Arrows indicate islets of Langerhans (scale bar = 1 mm). *I*: Mean surface of the islets of Langerhans was quantified. Values are means ± SEM. Differences between genotypes over time were analyzed by two-way ANOVA and Bonferroni post hoc test; differences between genotypes were calculated by Mann-Whitney test (*P = 0.05, **$P < 0.01$, ***$P < 0.001$). (A high-quality digital representation of this figure is available in the online issue.)

by LPL underlies the elevated plasma triglycerides. Consistently, hepatic mRNA levels of *apoCII* and *apoAV*, LPL activators, were markedly repressed (by 65 and 74%, respectively) in FXR$^{-/-}$*ob/ob* mice (Fig. 4*E*).

Hence, the repression of plasma triglyceride clearance regulators combined with the reduction of adipose tissue mass might result in the development of hypertriglyceridemia.

Total but not liver-specific FXR deficiency protects from diet-induced obesity and insulin resistance. To assess the impact of FXR deficiency in obesity in a model expressing functional leptin, lean FXR$^{-/-}$ and FXR$^{+/+}$ mice were fed a HFD for 20 weeks. Whereas FXR$^{+/+}$ mice rapidly gained weight upon HFD feeding, body weight remained significantly lower in FXR$^{-/-}$ mice (Fig. 5*A*). Consistently, plasma leptin levels were lower in FXR$^{-/-}$ mice (Fig. 5*B*). Plasma triglycerides were significantly higher in FXR$^{-/-}$ mice upon HFD feeding (Fig. 5*C*). FXR$^{-/-}$ mice further displayed lower blood glucose (Fig. 5*D*) and plasma insulin (Fig. 5*E*) concentrations and showed an improved glucose tolerance ($P < 0.0001$; two-way ANOVA; Fig. 5*F* and *G*). Hence, similar as in *ob/ob* mice, FXR deficiency protects from diet-induced obesity and insulin resistance.

To determine the contribution of hepatic FXR to the protection from diet-induced obesity and insulin resistance, liver-specific FXR$^{-/-}$ mice (LFXR$^{-/-}$) and wild-type littermates (LFXR$^{+/+}$) were fed a HFD for 9 weeks. Both LFXR$^{-/-}$ and LFXR$^{+/+}$ mice developed obesity (Fig. 6*A*) and displayed significantly elevated plasma leptin levels upon HFD feeding (Fig. 6*B*). LFXR$^{-/-}$ mice had significantly higher basal plasma triglycerides than LFXR$^{+/+}$ littermates but were unaffected by HFD feeding (Fig. 6*C*). HFD-fed

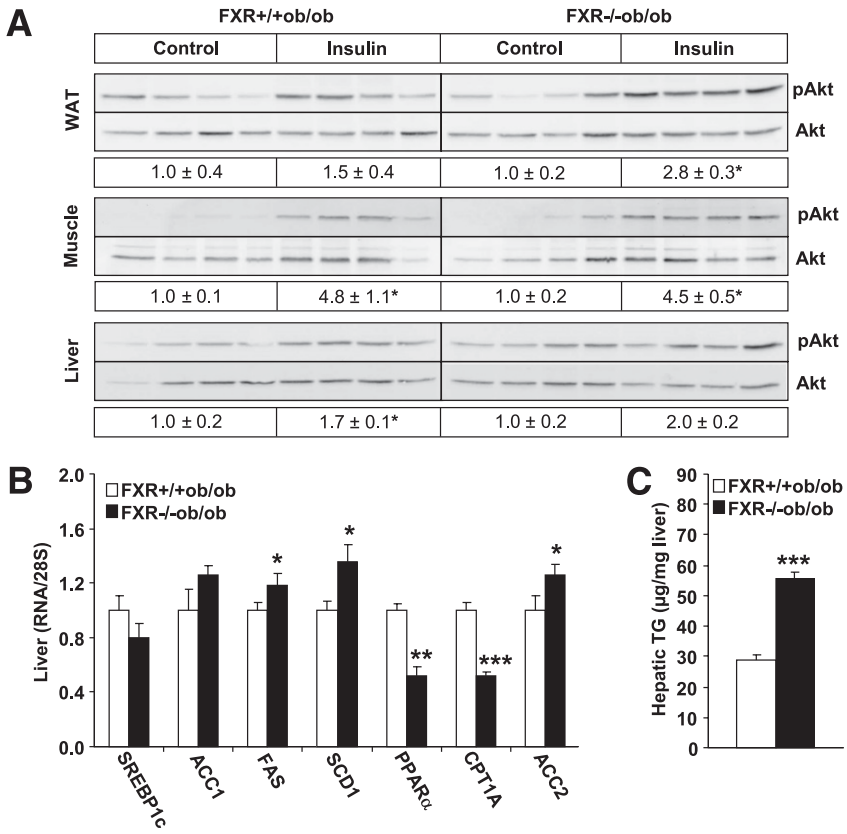

FIG. 3. FXR deficiency improves adipose tissue, but not hepatic insulin sensitivity in *ob/ob* mice. *A*: Female FXR$^{+/+}$*ob/ob* (13-week-old; white bars) and FXR$^{-/-}$*ob/ob* mice (black bars) (n = 4/group) were injected with either saline or insulin. Phosphorylation of Akt at Serine473 and total Akt protein expression was determined by Western blot and the signal quantified. *B*: Gene expression was measured by QPCR. *C*: Triglyceride content was determined enzymatically in livers of 20-week-old mice (n = 9 to 10/group). Values are means ± SEM. Differences between genotypes were calculated by Mann-Whitney test (*P < 0.05, **P < 0.01, ***P < 0.001). WAT, white adipose tissue; pAkt, Serine473-phosphorylated Akt; TG, triglyceride.

LFXR$^{-/-}$ and LFXR$^{+/+}$ mice became insulin resistant, displaying hyperglycemia (P < 0.0001; two-way ANOVA) (Fig. 6*D*) and elevated plasma insulin levels (Fig. 6*E*). In addition, the diet-induced glucose intolerance was similar in both genotypes (Fig. 6*F* and *G*). These findings indicate that liver-specific FXR deficiency does not protect from diet-induced obesity and insulin resistance.

Modulation of BA metabolism by sequestration does not affect glucose homeostasis in FXR$^{-/-}$*ob/ob* mice. FXR deficiency led to elevated plasma BA concentrations in genetic (394 ± 86 µM vs. 44 ± 13 µM; P < 0.001) and diet-induced obesity (119 ± 50 µM vs. 22 ± 6 µM). Because BA exert regulatory functions independent of FXR (17), we evaluated whether this increase may account for the observed alteration of body weight and glucose homeostasis.

The increased availability of plasma BA may lead to the activation of the TGR5 signaling pathway subsequently increasing energy expenditure in brown adipose tissue (BAT) (18). However, the expression of the TGR5 target genes *UCP1* and *D2* was decreased or unchanged, respectively, in BAT of FXR$^{-/-}$*ob/ob* compared with FXR$^{+/+}$*ob/ob* mice (Fig. 7*A*), indicating that TGR5 activity was not induced.

To assess whether reducing the elevated plasma BA levels in FXR$^{-/-}$*ob/ob* mice would affect glucose homeostasis, the BAS colesevelam was administered to FXR$^{-/-}$*ob/ob* and FXR$^{+/+}$*ob/ob* mice for 3 weeks. Colesevelam successfully reduced plasma BA concentrations in both genotypes by 80% already within 9 days of treatment (Fig. 7*B*). Body weight slightly but significantly increased with colesevelam treatment only in FXR$^{-/-}$*ob/ob* mice (Fig. 7*C*). Colesevelam decreased blood glucose levels in FXR$^{+/+}$*ob/ob*, but not FXR$^{-/-}$*ob/ob* mice (Fig. 7*D*). The glucose intolerance observed in untreated FXR$^{+/+}$*ob/ob* mice improved upon colesevelam treatment, whereas such effect was not observed in FXR$^{-/-}$*ob/ob* mice (Fig. 7*E* and *F*). However, both genotypes displayed increased plasma insulin concentrations upon treatment (Fig. 7*G*). Because BAS may lower glycemia by activating the incretin system (23), the expression of implicated intestinal genes was measured (Supplementary Table 2). *ProGIP*, coding for GIP, expression was repressed by FXR deficiency, whereas *proglucagon*, coding for GLP-1, was induced. Colesevelam moderately induced *PC1/3*, the enzyme activating both incretins, only in FXR$^{+/+}$*ob/ob* mice, unlikely explaining the observed improvement of glucose homeostasis. Indeed, plasma GLP-1 concentrations were not significantly different between genotypes and not enhanced by colesevelam treatment (data not shown). Thus, reducing plasma BA concentrations had no effect on glucose homeostasis in the absence of FXR, suggesting that the alterations of glucose metabolism observed in FXR deficiency are not mediated by circulating BA.

FXR deficiency differentially affects the abundance of long- and medium-chain triglyceride species in adipose tissue of lean and *ob/ob* mice. FXR deficiency improves glucose homeostasis in obesity, due at least in

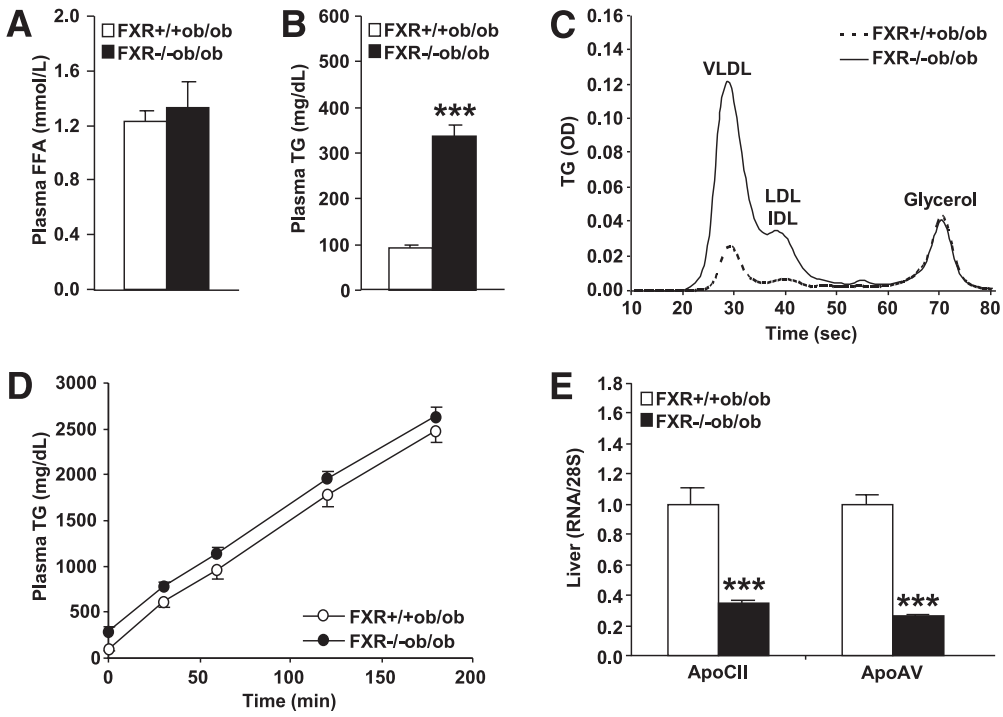

FIG. 4. FXR deficiency in *ob/ob* mice results in the accumulation of plasma triglycerides. *A* and *B*: Lipid parameters were measured in plasma of 12-week-old FXR$^{+/+}$*ob/ob* (white bars or circles) and FXR$^{-/-}$*ob/ob* mice (black bars or circles) (n = 9 to 10/group). *C*: Lipoprotein profiles were determined in plasma pools of 13-week-old mice. *D*: VLDL production was assessed in 13-week-old female mice (n = 8–10/group) by measuring plasma triglyceride concentrations subsequent to Tyloxapol injection. *E*: Gene expression was measured by QPCR in livers of 20-week-old mice (n = 9 to 10/group). Values are means ± SEM. Differences between genotypes were calculated by Mann-Whitney test (*P < 0.001). FFA, free fatty acid; OD, optical density; TG, triglyceride.**

part to an increase in adipose tissue insulin sensitivity. To investigate changes in adipose tissue lipid composition linked to FXR deficiency before the metabolic phenotype fully develops, high-resolution lipidomics was performed in subcutaneous adipose tissue from 6-week-old lean and *ob/ob* FXR$^{-/-}$ and FXR$^{+/+}$ mice.

Overall, 133 lipid species were quantified. Total phospholipid and sphingomyelin but not triglyceride content was significantly lower in obese than in lean mice (Supplementary Fig. 1). These lipid classes were unaffected by FXR deficiency. Of interest, a number of triglyceride species was differentially affected by FXR deficiency in lean and obese mice. Highly saturated medium-chain triglycerides were significantly higher in obese than lean FXR$^{+/+}$ mice (Fig. 8*A–C*) and tended to increase by FXR deficiency in both. In contrast, long-chain, unsaturated triglycerides, significantly elevated by obesity in FXR$^{+/+}$ mice, increased in lean but decreased in obese mice by FXR deficiency (Fig. 8*D–F*). Furthermore, long-chain triglycerides containing few double-bounds, which were similar between lean and obese FXR$^{+/+}$ mice, only decreased by FXR deficiency in obese mice (Fig. 8*G–I*).

PLS/DA revealed that the global subcutaneous adipose tissue lipid profiles clustered according to their genotype (Fig. 8*J*). Lipid profiles are significantly different between lean and obese mice whether deficient or not for FXR, visualized as a clear separation by the latent variable (LV)1 plotted on the x-axis. Interestingly, an additional separation of lean FXR$^{+/+}$ and obese FXR$^{-/-}$ from lean FXR$^{-/-}$ and obese FXR$^{+/+}$ mice by LV2 indicates that FXR deficiency modulates lipid profiles in an opposite manner in the lean versus obese background.

DISCUSSION

The nuclear receptor FXR is a metabolic regulator that controls BA and lipid as well as glucose and energy metabolism (2). FXR can exert direct transcriptional control or indirectly influence metabolic pathways by modulating the homeostasis of BA, which control metabolism also independent of FXR (17). The characteristics of FXR$^{-/-}$ mice, dyslipidemia (7–9), transient hypoglycemia upon fasting (8,10), peripheral insulin resistance (8,13), and reduced adipose tissue mass (8,15), reflect the importance of FXR for the maintenance of metabolic homeostasis. Yet, the impact of FXR deficiency on obesity and associated metabolic disorders has not been assessed. In the current study we demonstrate that FXR deficiency in murine models of genetic and diet-induced obesity attenuated weight gain by reducing adipose tissue mass. FXR deficiency further improved glucose homeostasis by enhancing peripheral glucose disposal and increasing adipose tissue insulin sensitivity. This improvement is not mediated by hepatic FXR, since liver insulin sensitivity was unchanged and liver-specific FXR$^{-/-}$ mice were not protected from diet-induced obesity and insulin resistance. The administration of the BAS colesevelam, which reduced the elevated plasma BA levels resulting from FXR deficiency in obesity, further revealed that the improved glucose homeostasis was independent of BA-mediated pathways. FXR deficiency thus exerts a beneficial effect on body weight development and glucose homeostasis in obesity.

FXR$^{-/-}$ mice display peripheral insulin resistance, but reported results on the liver are contradicting (8,13,31). Surprisingly, we observed an improvement of glucose homeostasis by FXR deficiency in genetic and diet-induced

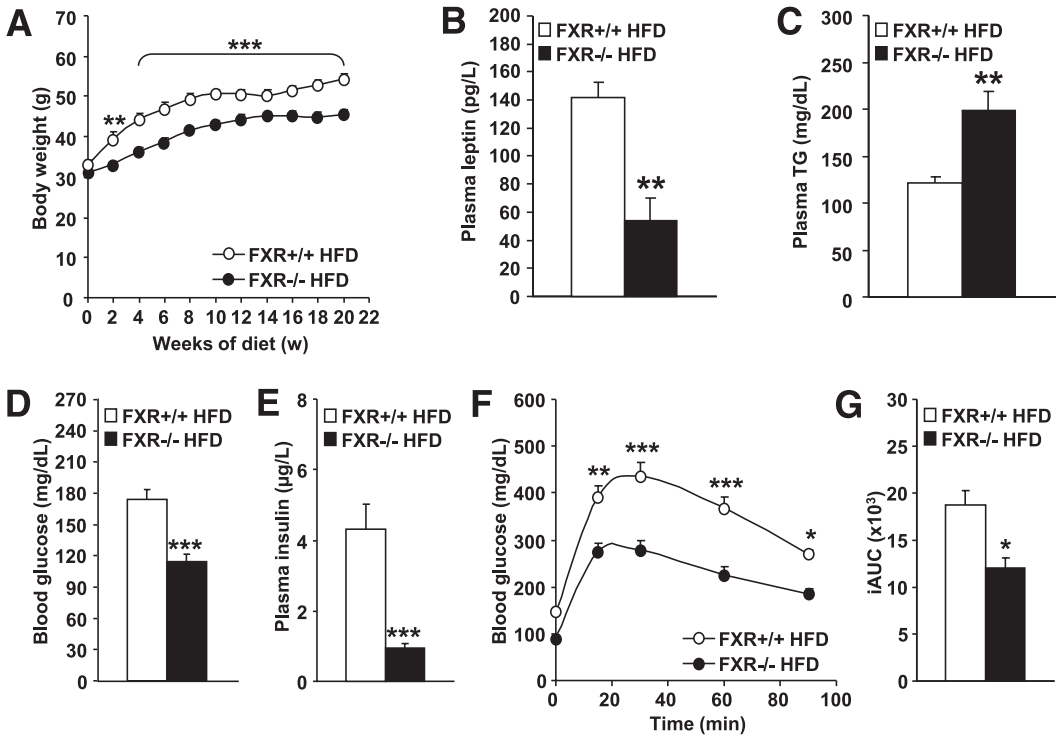

FIG. 5. FXR deficiency protects from diet-induced obesity and insulin resistance. $FXR^{+/+}$ (white bars or circles) and $FXR^{-/-}$ mice (black bars or circles) (n = 7–11/group) were fed a HFD for 20 weeks. *A*: Body weight was monitored weekly (n = 7–11/group). Significance of the overall effect of genotype ($P < 0.0001$) and age ($P < 0.0001$) as well as their interaction ($P < 0.0001$) was calculated by two-way ANOVA. Plasma leptin (*B*), plasma triglyceride (TG) (*C*), blood glucose (*D*), and plasma insulin (*E*) were determined at the end of the feeding period (n = 4–9/group). Blood glucose excursion (*F*) and integrated AUC (*G*) after administration of an intraperitoneal glucose bolus (1 g/kg glucose) were measured at the end of the feeding period (n = 6–9/group). Significance of the overall effect of genotype ($P < 0.0001$) and time ($P < 0.0001$) was calculated by two-way ANOVA. Values are means ± SEM. Differences between genotypes over time were analyzed by two-way ANOVA and Bonferroni post hoc test; differences between genotypes were calculated by Mann-Whitney test (*$P < 0.05$, **$P < 0.01$, ***$P < 0.001$).

obesity, revealing a differential role for FXR in glucose homeostasis in basal (lean) and challenged (obese) metabolic conditions. The reduction of hyperglycemia in $FXR^{-/-}$ *ob/ob* mice resulted from an increased peripheral glucose disposal associated with an improved adipose tissue insulin sensitivity. This suggests that FXR in adipose tissue contributes to the dysregulation of glucose metabolism in obesity. Hypertrophic adipocytes develop insulin resistance (32). Hence the reduced adipocyte size in $FXR^{-/-}$ *ob/ob* mice (16) might explain the increased insulin sensitivity. In addition to adipose tissue, skeletal muscle is the main peripheral tissue accounting for glucose uptake. However, the insulin signaling response in skeletal muscle was unaffected by FXR deficiency. Moreover, FXR is not expressed in skeletal muscle (8) and muscle mass strongly reduced in genetic obesity. We can therefore exclude the involvement of skeletal muscle in the FXR deficiency–mediated changes of glucose homeostasis.

FXR exerts a key function in the control of hepatic glucose and lipid metabolism (2). In hepatic insulin resistance, increased endogenous glucose production contributes to hyperglycemia and continuous insulin-mediated activation of lipogenesis leads to hyperlipidemia and may cause a fatty liver (32). In contrast with adipose tissue, FXR deficiency did not improve hepatic insulin sensitivity in genetic obesity and liver-specific FXR deficiency did not protect from diet-induced insulin resistance, a rather surprising result regarding the importance of hepatic FXR for the metabolic control of lean mice. Furthermore, hepatic steatosis often associated with hepatic insulin resistance increased in $FXR^{-/-}$*ob/ob* mice because of a repression of β-oxidation. Moreover, the repression of hepatic LPL cofactors led to an impaired intravascular triglyceride clearance resulting in elevated plasma triglycerides. Overall, the changes in lipid metabolism appear to be primarily a result of altered liver function, whereas the results on insulin sensitivity emphasize a role for nonhepatic FXR in the dysregulation of glucose homeostasis in obesity, most probably in adipose tissue.

Several studies have shown that FXR controls adipocyte differentiation and function (8,15,16). FXR expression occurs early and transiently during adipocyte development, inhibiting the Wnt/β-catenin pathway, thus allowing optimal PPAR-γ activation (16). Because the lack of hepatic FXR does not seem to mediate the improvement of glucose homeostasis in obesity, it would be of great interest to study adipose tissue-specific FXR deficiency in obesity. Unfortunately, in the currently available mouse models Cre recombinase expression is driven by promoters from late and/or nonspecific adipocyte genes (i.e., adiponectin or *aP2*), rendering them inappropriate to study the influence of genes acting earlier in the differentiation process, such as *FXR*.

FXR deficiency in obesity was associated with elevated plasma BA levels. BA have been reported to improve glucose homeostasis independent of FXR by TGR5-mediated stimulation of GLP-1 secretion (19,20). The administration of the BAS colesevelam to *ob/ob* mice successfully reduced plasma BA concentrations but had no effect on glucose homeostasis in the absence of FXR. Thus, elevated

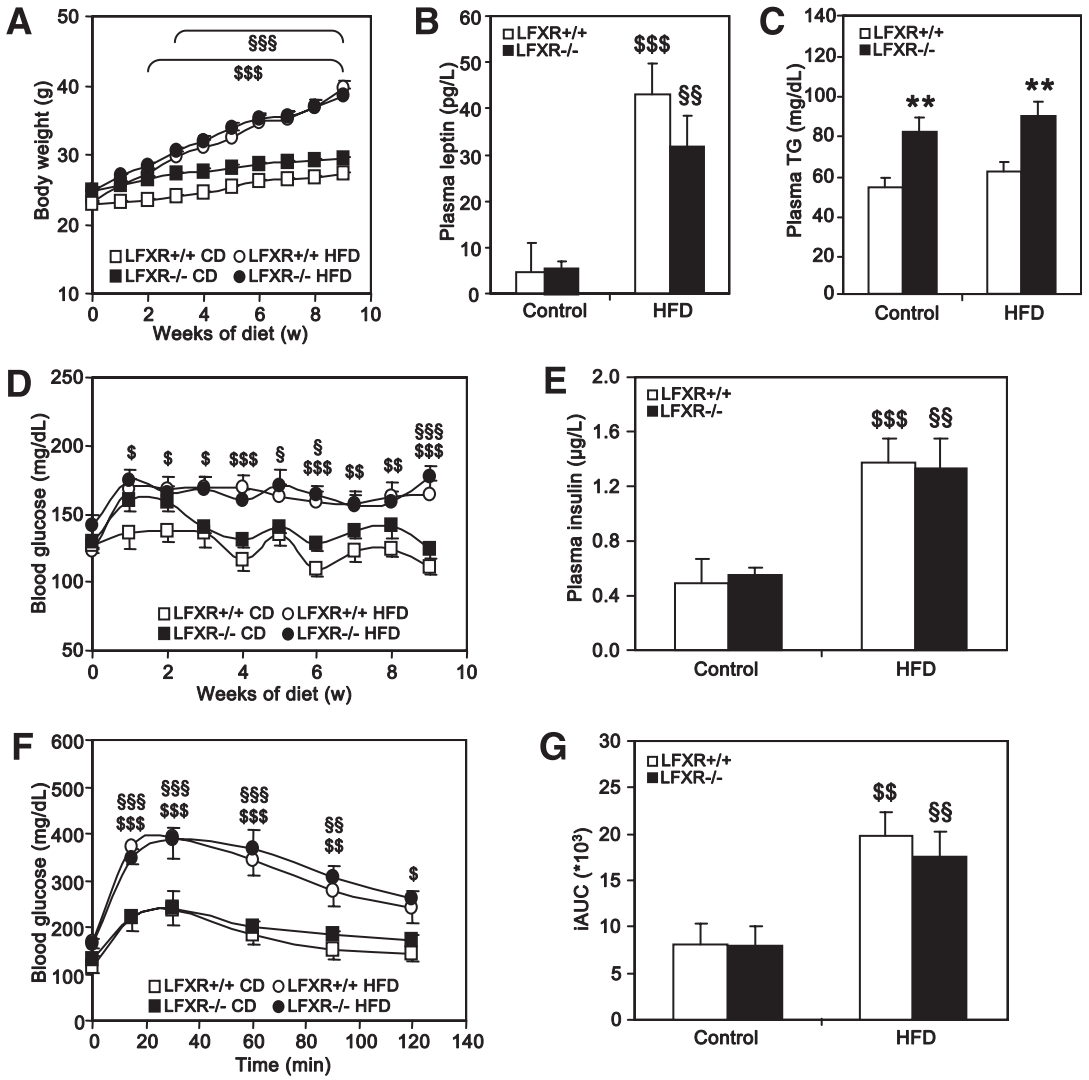

FIG. 6. Liver-specific FXR deficiency does not protect from diet-induced obesity and insulin resistance. LFXR$^{-/-}$ mice and LFXR$^{+/+}$ littermates (n = 7–12/group) were fed a HFD or a control diet (CD) for 10 weeks (LFXR$^{+/+}$, white bars and symbols; LFXR$^{-/-}$, black bars and symbols). *A*: Body weight was monitored weekly. Significance of the effect of diet ($P < 0.0001$) and age ($P < 0.0001$) as well as their interaction ($P < 0.0001$) was calculated by two-way ANOVA. Plasma leptin (*B*) and plasma triglyceride (TG) (*C*) were determined at the end of the feeding period. *D*: Fasting blood glucose was measured weekly. Significance of the overall effect of diet ($P < 0.0001$) and age ($P < 0.0001$) as well as their interaction (P = 0.0217) was calculated by two-way ANOVA. *E*: Plasma insulin was measured after 6 weeks of feeding. Blood glucose excursion (*F*) and integrated AUC (*G*) after administration of an intraperitoneal glucose bolus (1 g/kg glucose) were measured after 5 weeks of feeding (n = 6/group). Values are means ± SEM. Differences between diet groups over time were analyzed by two-way ANOVA and Bonferroni post hoc test; differences between genotypes or diet groups were calculated by Mann-Whitney test. *Compares genotypes of the same diet group; $compares diet groups for LFXR$^{+/+}$; §compares diet groups for LFXR$^{-/-}$ ($ or §$P < 0.05$; **, $$, or §§$P < 0.01$; $$$ or §§§$P < 0.001$).

circulating BA in FXR deficiency do not mediate the observed improvement in glucose homeostasis. BAS improve glycemic control in type 2 diabetes, also partly via a TGR5-mediated increase of GLP-1 (22,23). However, GLP-1 secretion was unaffected by genotype or colesevelam treatment. Thus, the observed FXR-dependent improvement of glycemic control by colesevelam in *ob/ob* mice suggests that FXR-mediated pathways contribute to the beneficial effect of BAS.

Contradictory to our observation that FXR deficiency is beneficial for glucose homeostasis in obesity, FXR activation has been shown to improve insulin resistance in rodent models of diabetes (8,31,33). The reason for this apparent inconsistency is currently unclear. However, the pharmacological activation of a nuclear receptor does not necessarily have opposite effects than the knockout of its expression. The specific pharmacodynamics of the used compounds may also affect FXR in a tissue-specific manner (sBARM effect), whereas our study focused on whole-body FXR deficiency.

Both genetic and diet-induced obesity are attenuated in the absence of FXR. FXR deficiency leads to reduced adipose tissue mass (8,15,16) and adipocyte size (16) in lean and *ob/ob* mice, limiting energy storage capacity. Because food intake and energy expenditure only tended to decrease in FXR$^{-/-}$*ob/ob* mice, the decreased adipose tissue mass most likely accounts for the reduced weight gain. With regard to the moderate decrease in energy expenditure, a central effect of FXR seems unlikely, additionally since FXR expression in hypothalamus is only very weak (34). Furthermore, the lack of TGR5 target gene induction in BAT of FXR$^{-/-}$*ob/ob* mice argues against the implication of a TGR5-cAMP-D2–mediated mechanism (18). If the reduced body weight was a direct effect of a decreased food

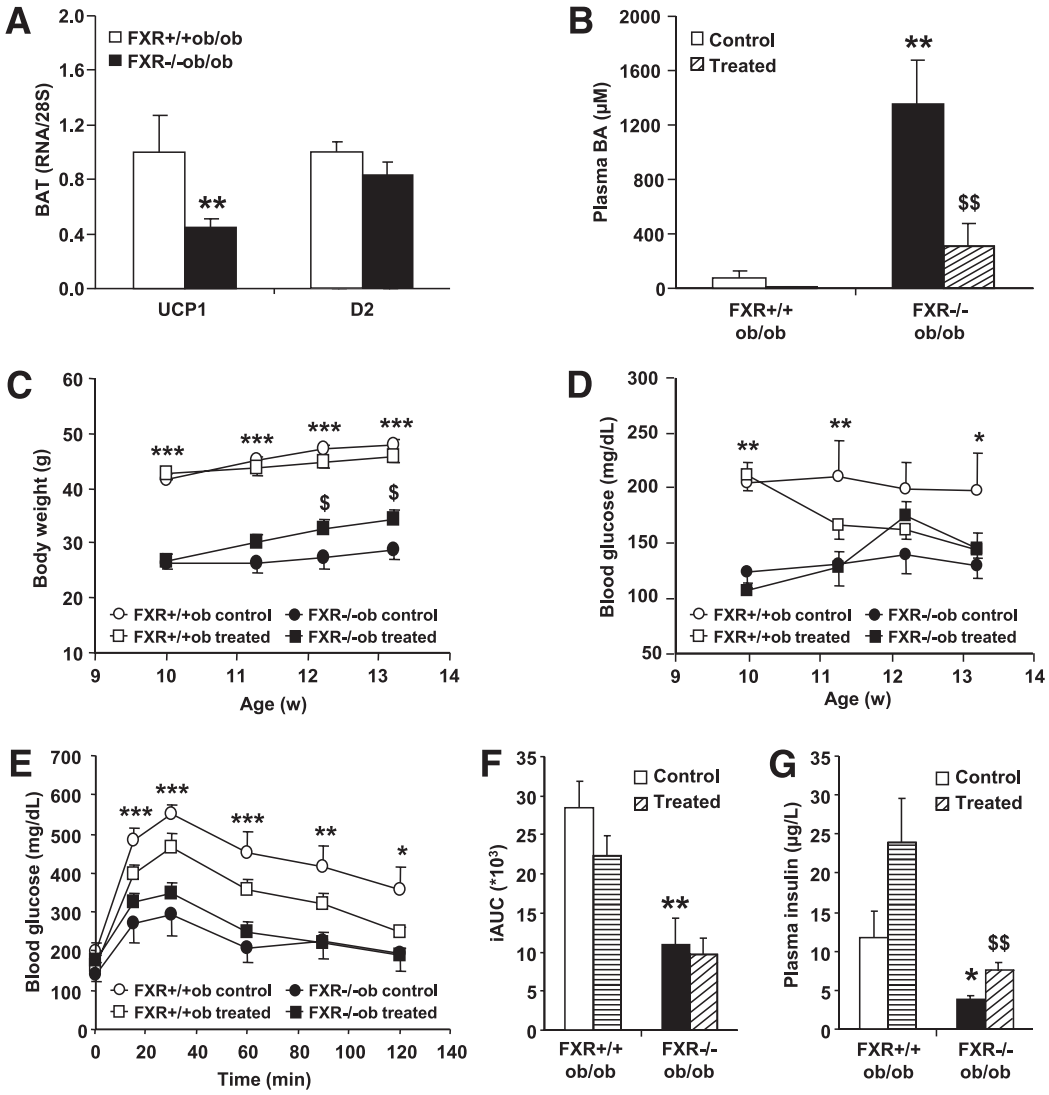

FIG. 7. Modulation of BA metabolism does not affect glucose homeostasis in FXR$^{-/-}$*ob/ob* mice. FXR$^{+/+}$*ob/ob* and FXR$^{-/-}$*ob/ob* mice (10 weeks old) were administered 2% colesevelam mixed in the diet or plain diet for 3 weeks (n = 13/group) (FXR$^{+/+}$*ob/ob* control, white bars or circles; FXR$^{+/+}$ *ob/ob* treated, horizontally hatched bars or white squares; FXR$^{-/-}$*ob/ob* control, black bars or circles; FXR$^{-/-}$*ob/ob* treated, diagonally hatched bars or black squares). *A*: TGR5 target gene expression was measured by QPCR in BAT of 20-week-old mice (n = 9 to 10/group). *B*: Plasma BA were measured after 9 days of treatment. *C*: Body weight was monitored weekly during the treatment period. Significance of the overall effect of treatment ($P < 0.0001$) and age ($P = 0.0002$) was calculated by two-way ANOVA. *D*: Fasting blood glucose was determined weekly during the treatment period. Blood glucose excursion (*E*) and integrated AUC (*F*) after administration of an intraperitoneal glucose bolus (1 g/kg glucose) were measured at the end of the treatment period. *G*: Plasma insulin was measured at the end of the treatment period. Values are means ± SEM. Differences between treatment groups over time were analyzed by two-way ANOVA and Bonferroni post hoc test; differences between genotypes or treatment groups were calculated by Mann-Whitney test. *Compares genotypes of the same treatment group; $compares treatment groups of the same genotype (* or $$P < 0.05$, ** or $$P < 0.01$, ***$P < 0.001$).

intake in the hyperphagic model of FXR$^{-/-}$*ob/ob* mice, the hepatic triglyceride content would have also been reduced and not elevated as observed.

Interestingly, the analysis of adipose tissue lipid profiles by lipidomics revealed a differential alteration of certain triglyceride classes in lean and obese mice by FXR deficiency, e.g., long-chain, unsaturated triglycerides are lowered by FXR deficiency in obese but increased in lean mice. This observation demonstrates that FXR deficiency specifically and opposingly affects adipose tissue metabolism as it does glucose homeostasis in lean and obese conditions.

Overall, in contrast with lean mice, FXR deficiency in obesity improves energy and glucose homeostasis. The selective inhibition of FXR activity may thus be an appealing option for the therapy of obesity and the related dysregulation of glucose homeostasis.

ACKNOWLEDGMENTS

This study was supported by the European Union Grant HEPADIP (No. 018734), the Agence Nationale de la Recherche (No. A05056GS), and COST (Action BM0602).

The authors are grateful to Daiichi Sankyo for providing colesevelam and an unrestricted scientific grant. No other potential conflicts of interest relevant to this article were reported.

J.P. performed experiments and wrote the manuscript. M.A., J.H.M.S., I.P., H.D., V.R.V., J.D., E.B., T.H.v.D., A.L., E.D., and M.D. performed experiments and contributed to

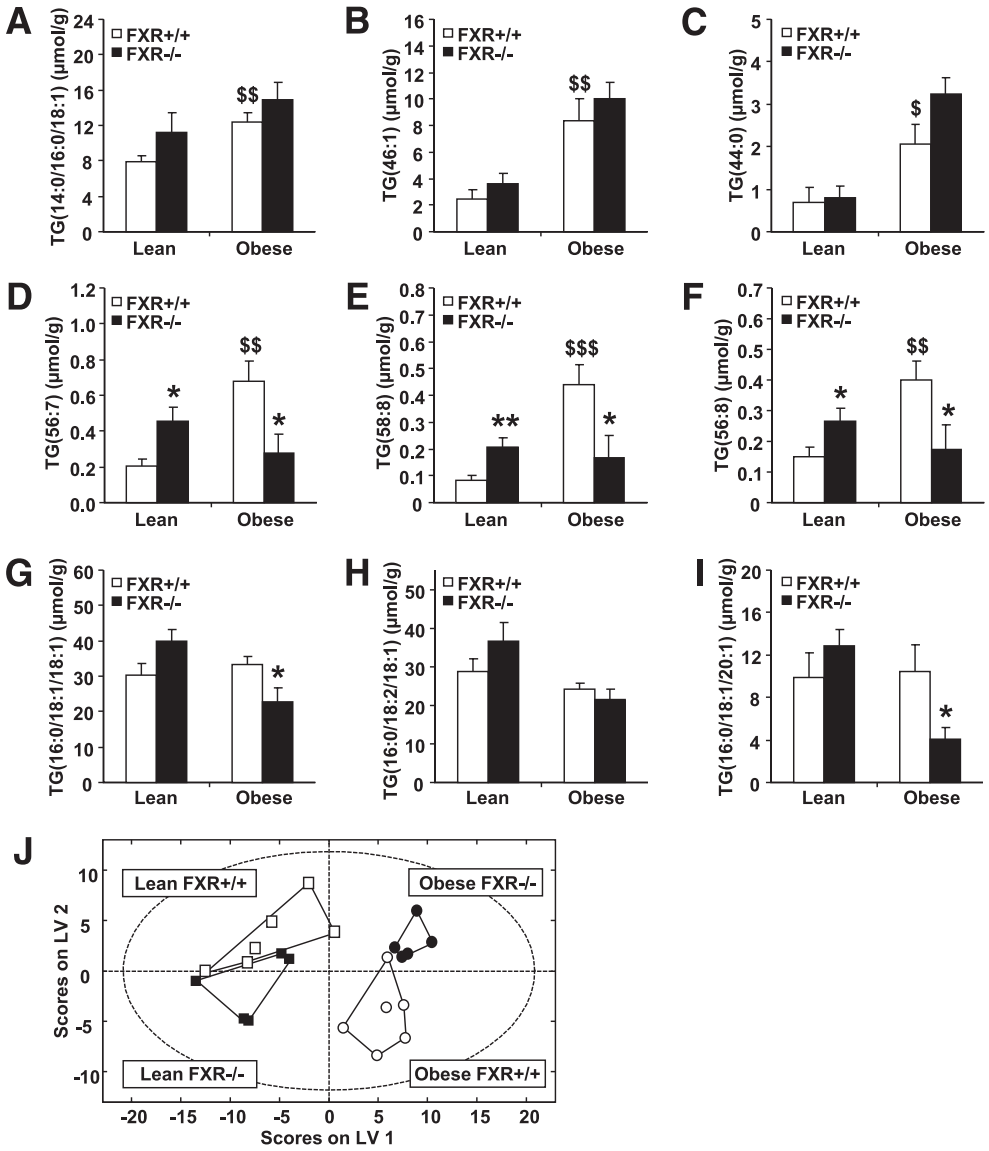

FIG. 8. FXR deficiency differentially affects the abundance of long-chain, unsaturated triglyceride (TG) species in adipose tissue of lean and obese mice. Lipidomic analysis was performed in white adipose tissue of 6-week-old FXR$^{+/+}$*ob/ob*, FXR$^{-/-}$*ob/ob* mice, as well as lean FXR$^{+/+}$ and FXR$^{-/-}$ littermates (lean FXR$^{+/+}$, white bars or squares; lean FXR$^{-/-}$, black bars or squares; obese FXR$^{+/+}$, white bars or circles; obese FXR$^{-/-}$, black bars or circles). Representative data for *A–C*: Medium-chain triglycerides with a high saturation level. *D–F*: Long-chain, highly unsaturated triglycerides. *G–I*: Long-chain triglycerides containing few double-bounds. *J*: PLS/DA of all measured lipid species. Values are means ± SEM. Differences between genotypes were calculated by one-way ANOVA and Student *t* test. *Compares the effect of leptin-deficiency; $compares the effect of FXR deficiency (* or $*P* < 0.05, ** or $$*P* < 0.01, or $$$*P* <0.001).

discussion. S.L., F.J.G., and M.O. contributed to discussion and reviewed the manuscript. B.C. performed experiments, contributed to discussion, and reviewed the manuscript. F.K. contributed to discussion and reviewed the manuscript. S.C. performed experiments, contributed to discussion, and reviewed the manuscript. B.S. contributed to discussion and wrote, reviewed, and edited the manuscript.

REFERENCES

1. Cornier MA, Dabelea D, Hernandez TL, et al. The metabolic syndrome. Endocr Rev 2008;29:777–822
2. Lefebvre P, Cariou B, Lien F, Kuipers F, Staels B. Role of bile acids and bile acid receptors in metabolic regulation. Physiol Rev 2009;89:147–191
3. Prawitt J, Caron S, Staels B. How to modulate FXR activity to treat the metabolic syndrome. Drug Discov Today Dis Mech 2009;6:e55–e64
4. Watanabe M, Houten SM, Wang L, et al. Bile acids lower triglyceride levels via a pathway involving FXR, SHP, and SREBP-1c. J Clin Invest 2004;113:1408–1418
5. Kast HR, Nguyen CM, Sinal CJ, et al. Farnesoid X-activated receptor induces apolipoprotein C-II transcription: a molecular mechanism linking plasma triglyceride levels to bile acids. Mol Endocrinol 2001;15:1720–1728
6. Claudel T, Inoue Y, Barbier O, et al. Farnesoid X receptor agonists suppress hepatic apolipoprotein CIII expression. Gastroenterology 2003;125:544–555
7. Sinal CJ, Tohkin M, Miyata M, Ward JM, Lambert G, Gonzalez FJ. Targeted disruption of the nuclear receptor FXR/BAR impairs bile acid and lipid homeostasis. Cell 2000;102:731–744
8. Cariou B, van Harmelen K, Duran-Sandoval D, et al. The farnesoid X receptor modulates adiposity and peripheral insulin sensitivity in mice. J Biol Chem 2006;281:11039–11049
9. Lambert G, Amar MJA, Guo G, Brewer HB Jr, Gonzalez FJ, Sinal CJ. The farnesoid X-receptor is an essential regulator of cholesterol homeostasis. J Biol Chem 2003;278:2563–2570

10. van Dijk TH, Grefhorst A, Oosterveer MH, et al. An increased flux through the glucose 6-phosphate pool in enterocytes delays glucose absorption in Fxr-/- mice. J Biol Chem 2009;284:10315–10323
11. Duran-Sandoval D, Cariou B, Percevault F, et al. The farnesoid X receptor modulates hepatic carbohydrate metabolism during the fasting-refeeding transition. J Biol Chem 2005;280:29971–29979
12. Cariou B, van Harmelen K, Duran-Sandoval D, et al. Transient impairment of the adaptive response to fasting in FXR-deficient mice. FEBS Lett 2005; 579:4076–4080
13. Ma K, Saha PK, Chan L, Moore DD. Farnesoid X receptor is essential for normal glucose homeostasis. J Clin Invest 2006;116:1102–1109
14. Stayrook KR, Bramlett KS, Savkur RS, et al. Regulation of carbohydrate metabolism by the farnesoid X receptor. Endocrinology 2005;146:984–991
15. Rizzo G, Disante M, Mencarelli A, et al. The farnesoid X receptor promotes adipocyte differentiation and regulates adipose cell function in vivo. Mol Pharmacol 2006;70:1164–1173
16. Abdelkarim M, Caron S, Duhem C, et al. The farnesoid X receptor regulates adipocyte differentiation and function by promoting peroxisome proliferator-activated receptor-gamma and interfering with the Wnt/beta-catenin pathways. J Biol Chem 2010;285:36759–36767
17. Thomas C, Pellicciari R, Pruzanski M, Auwerx J, Schoonjans K. Targeting bile-acid signalling for metabolic diseases. Nat Rev Drug Discov 2008;7:678–693
18. Watanabe M, Houten SM, Mataki C, et al. Bile acids induce energy expenditure by promoting intracellular thyroid hormone activation. Nature 2006;439:484–489
19. Katsuma S, Hirasawa A, Tsujimoto G. Bile acids promote glucagon-like peptide-1 secretion through TGR5 in a murine enteroendocrine cell line STC-1. Biochem Biophys Res Commun 2005;329:386–390
20. Thomas C, Gioiello A, Noriega L, et al. TGR5-mediated bile acid sensing controls glucose homeostasis. Cell Metab 2009;10:167–177
21. Staels B, Handelsman Y, Fonseca V. Bile acid sequestrants for lipid and glucose control. Curr Diab Rep 2010;10:70–77
22. Chen L, McNulty J, Anderson D. Cholestyramine reverses hyperglycemia and enhances glucose-stimulated glucagon-like peptide 1 release in Zucker diabetic fatty rats. J Pharmacol Exp Ther 2010;334:164–170
23. Shang Q, Saumoy M, Holst JJ, Salen G, Xu G. Colesevelam improves insulin resistance in a diet-induced obesity (F-DIO) rat model by increasing the release of GLP-1. Am J Physiol Gastrointest Liver Physiol 2010;298: G419–G424
24. Murphy GM, Billing BH, Baron DN. A fluorimetric and enzymatic method for the estimation of serum total bile acids. J Clin Pathol 1970;23:594–598
25. Elia M, Livesey G. Energy expenditure and fuel selection in biological systems: the theory and practice of calculations based on indirect calorimetry and tracer methods. World Rev Nutr Diet 1992;70:68–131
26. Laskewitz AJ, van Dijk TH, Bloks VW, et al. Chronic prednisolone treatment reduces hepatic insulin sensitivity while perturbing the fed-to-fasting transition in mice. Endocrinology 2010;151:2171–2178
27. Popescu IR, Helleboid-Chapman A, Lucas A, et al. The nuclear receptor FXR is expressed in pancreatic beta-cells and protects human islets from lipotoxicity. FEBS Lett 2010;584:2845–2851
28. Chomczynski P, Sacchi N. Single-step method of RNA isolation by acid guanidinium thiocyanate-phenol-chloroform extraction. Anal Biochem 1987;162:156–159
29. Laaksonen R, Katajamaa M, Päivä H, et al. A systems biology strategy reveals biological pathways and plasma biomarker candidates for potentially toxic statin-induced changes in muscle. PLoS ONE 2006;1:e97
30. Kotronen A, Yki-Järvinen H. Fatty liver: a novel component of the metabolic syndrome. Arterioscler Thromb Vasc Biol 2008;28:27–38
31. Zhang Y, Lee FY, Barrera G, et al. Activation of the nuclear receptor FXR improves hyperglycemia and hyperlipidemia in diabetic mice. Proc Natl Acad Sci USA 2006;103:1006–1011
32. Biddinger SB, Kahn CR. From mice to men: insights into the insulin resistance syndromes. Annu Rev Physiol 2006;68:123–158
33. Cipriani S, Mencarelli A, Palladino G, Fiorucci S. FXR activation reverses insulin resistance and lipid abnormalities and protects against liver steatosis in Zucker (fa/fa) obese rats. J Lipid Res 2010;51:771–784
34. Gofflot F, Chartoire N, Vasseur L, et al. Systematic gene expression mapping clusters nuclear receptors according to their function in the brain. Cell 2007;131:405–418